Braz J Phys (2014) 44:415–425
DOI 10.1007/s13538-014-0219-5

SOCIEDADE BRASILEIRA DE FÍSICA

PARTICLES AND FIELDS

Particle Acceleration by Shocks in Supernova Remnants

Anthony Raymond Bell

Received: 28 April 2014 / Published online: 28 May 2014

Abstract Particle acceleration occurs on a range of scales from AU in the heliosphere to Mpc in clusters of galaxies and to energies ranging from MeV to exaelectronvolt (EeV). A number of acceleration processes have been proposed, but diffusive shock acceleration (DSA) is widely invoked as the predominant mechanism. DSA operates on all these scales and probably to the highest energies. DSA is simple, robust and predicts a universal spectrum. However, there are still many unknowns regarding particle acceleration. This paper focuses on the particular question of whether supernova remnants (SNR) can produce the Galactic cosmic ray (CR) spectrum up to the knee at a few petaelectronvolt (PeV). The answer depends in large part on the detailed physics of diffusive shock acceleration.

Keywords Cosmic rays · Particle acceleration · Magnetic field · Supernova remnants

1 Introduction

Energetic particles are prevalent throughout the universe, ranging from MeV particles in the heliosphere to teraelectronvolt (TeV) particles in supernova remnants to exaelectronvolt (EeV) particles that almost certainly originate beyond our own Galaxy. At low energies within the heliosphere, they are detected by satellites, while at high energies, they arrive at the Earth as cosmic rays (CR). CR in distant objects are detected from radio to γ-ray wavebands by means of electron synchrotron and inverse Compton emission or γ-ray emission from pion-producing collisions between cosmic rays and background protons. The presence of CR in supernova remnants (SNR) with energies of 100s of TeV is proved by the detection at the Earth of γ-rays with energies up to nearly 100 TeV arriving from the direction of the source [3, 4]. Particle acceleration is known to be efficient because the Galactic cosmic ray energy density can only be generated if a significant fraction of the energy of supernova explosions is given to energetic particles. Blandford and Eichler [14] estimate an efficiency of a few percent. Initial explanations of CR acceleration centred on the second-order Fermi process [25] by which CR gains energy from elastic collisions with magnetic field structures in motion in the interstellar medium (ISM). If the typical velocity of a magnetic structure is u, the excess probability of a CR encountering it head-on rather than tail-on is proportional to u/c with a fractional increase in CR energy of order u/c on a head-on encounter, so the process is second order in u/c. The second-order process probably contributes to particle acceleration, but it was realised in the late 1970s that a more rapid first-order process, known as diffusive shock acceleration (DSA), occurs wherever there are strong releases of energy that produce blast waves [6, 7, 15, 33]. CR diffusion back and forth across a strong shock produces a fractional energy gain of order u/c on each crossing, where u is the shock velocity. On average, each CR crosses the shock c/u times before escaping downstream of the shock, with a probability $(1-u/c)^m$ of escaping after at least m shock crossings. A simple derivation shows that a E^{-2} differential energy spectrum arises naturally from DSA at a strong shock. Its advantages as a theoretical explanation of particle acceleration are that a large part of a supernova energy release is processed through the expanding shock front, the energy spectrum matches observation reasonably well, and high

A. R. Bell (✉)
Clarendon Laboratory, University of Oxford,
Oxford OX1 3PU, UK
e-mail: t.bell1@physics.ox.ac.uk

acceleration efficiency appears likely. The conclusion was soon drawn that DSA at supernova shocks is probably the main source of Galactic CR. The highest-energy (EeV) CR may possibly be produced in AGN, radio galaxies or GRB where much of the available energy is processed through high-velocity shocks or shocks with a large spatial extent.

DSA offers a generic explanation of astrophysical particle acceleration, but the explanation has not been, and still is not, completely straightforward. In two crucial papers, Lagage and Cesarsky [36, 37] reasoned that DSA at SNR shocks appeared incapable of accelerating protons to peta-electronvolt (PeV) energies. Since the Galactic CR energy spectrum extends from gigaelectronvolt (GeV) to a few PeV as a nearly straight power law, it seems necessary that the same mechanism accelerating CR to TeV should also be accelerating CR from TeV to PeV. Because the spectrum steepens rather than flattens in a 'knee' at a few PeV, the spectrum beyond the knee cannot easily be explained as the coincidental meeting of different populations above and below the knee. So the same process is probably responsible for CR acceleration beyond the knee, although the problem is alleviated if CR beyond the knee are heavy nuclei rather than protons.

This review is principally concerned with the particular question of whether supernova remnants (SNR) accelerate CR to the knee in the Galactic energy spectrum at a few PeV. More broadly based reviews of diffusive shock acceleration or with a different focus are given by Drury [21], Blandford and Eichler [14], Jones and Ellison [31], Malkov and Drury [41] and Bell [10].

2 The Maximum CR Energy

In DSA at a strong shock propagating at velocity u, the CR energy increases on average by a fraction u/c each time the CR cycles from upstream to downstream and back to upstream. Consequently, a CR must cross the shock typically $(c/u)\log(E_2/E_1)$ times for acceleration from energy E_1 to E_2. Krymsky [34] derived a time λ/u_d, where λ is the CR mean free path and u_d is the downstream velocity relative to the shock, for CR to cycle between upstream and downstream. Allowing for different conditions upstream and downstream, the complete mean cycle time between upstream and downstream is $\tau_\mathrm{cycle} = 4[D_\mathrm{u}/u + D_\mathrm{d}/u_\mathrm{d}]/c$ [36, 37], where D_u and D_d are the upstream and downstream CR diffusion coefficients, respectively, and $u_\mathrm{d} = u/4$ for a strong shock. The ratio of τ_cycle to the age of the SNR indicates that CR reach a maximum energy of typically $\sim 10^{13}$ eV, which falls 100 times short of the energy of the knee. The Lagage and Cesarsky limit can be derived as follows.

Balance between diffusion away from the shock upstream and advection back to the shock at velocity u creates an exponential CR precursor upstream of the shock with a scale height $L = D_\mathrm{u}/u$. The number of CR in the precursor per unit shock area is nD_u/u where n is the CR number density at the shock. CR cross the shock at a rate $nc/4$, so the average time a CR spends upstream between crossings is $4D_\mathrm{u}/cu$. The time spent downstream is similarly $4D_\mathrm{d}/cu_\mathrm{d}$ giving the total cycle time. At each cycle, the CR energy increases by a fraction u/c on average, so the characteristic time for energy gain is $\tau_\mathrm{gain} = (c/u)\tau_\mathrm{cycle} = 4(D_\mathrm{u} + 4D_\mathrm{d})/u^2$.

Blasi and Amato [16] find best fits for the Galactic diffusion coefficient of the form $D = D_{28}10^{28}(E/3\mathrm{GeV})^\delta$ cm^{2}s^{-1} with $D_{28} = 1.33H_\mathrm{kpc}$ for $\delta = 1/3$ or $D_{28} = 0.55H_\mathrm{kpc}$ for $\delta = 0.6$, where H_kpc is the height of the Galactic halo in kpc. If these diffusion coefficients were to apply to diffusive shock acceleration in SNR expanding at 5,000 km s^{-1}, the acceleration time at GeV energies would be $\sim 10^4$ years. It would take an impossibly long time for CR to reach PeV energies, between 10^6 and 10^8 years, by which time the shock would have slowed substantially ($u \ll$ 5,000 km s^{-1}) or dissolved into the interstellar medium. The long estimated acceleration time reflects the large mean free path for CR scattering in the interstellar medium. Fortunately, the large currents of streaming CR close to the SNR excite plasma instabilities that drive fluctuations in the magnetic field and increase CR scattering. Two especially effective CR-driven plasma instabilities are a resonant instability [7, 35, 39, 56–58, 68], in which the CR resonantly excite the Alfven waves, and a nonresonant instability [8], in which a purely growing mode is strongly driven under conditions found in young SNR. Throughout this paper, the first of these two instabilities will be referred to as the 'Alfven instability' because it drives the Alfven waves. The second instability will be referred to as the 'nonresonant hybrid (NRH) instability' because the mode is not spatially resonant with the CR Larmor radius and because it is hybrid in the sense that kinetic CR interact with a fluid background plasma. These instabilities will be discussed below. Other instabilities such as the Drury instability [23], the firehose instability and other long-wavelength instabilities [19, 47, 48, 53] probably also play a role in perturbing the upstream magnetic field and reducing the diffusion coefficient. Additionally, magnetic field amplification may take place downstream of the shock due to vorticity induced by density inhomogeneities in the plasma overtaken by the shock [26, 69], but amplification may occur too far downstream to contribute to CR acceleration at the shock [27].

Plasma instabilities can generate magnetic structures that scatter CR, but the mean free path for scattering in a magnetic field cannot be smaller than the Larmor radius $r_g =$

p/eB, where p is the CR momentum and B is the magnetic field upstream of the shock in tesla. The upstream diffusion coefficient D_u is consequently at least $r_g c/3 = E/3B$, where E is the energy in electronvolt (eV). The perpendicular component of the magnetic field is compressed by a factor of four at the shock, so a reasonable assumption is that $D_d \sim D_u/4$ within a numerical factor of order 1. If $D_d = D_u/4$, the downstream cycle time $4D_d/c(u/4)$ is equal to the upstream cycle time $4D_u/cu$, and the total cycle time is $\tau_{cycle} = 8E/3Bu$. Under this assumption, the characteristic time for energy gain is $\tau_{gain} = 8E/3Bu^2$. Setting the acceleration time equal to the SNR expansion time R/u where R is the SNR radius gives a maximum energy $E_{max} = 3uBR/8$ eV, which is equivalent to

$$E_{max} = 1.2 \times 10^{13} u_7 B_{\mu G} R_{pc} \text{ eV} \quad (1)$$

where $B_{\mu G}$ is the magnetic field in microgauss, R_{pc} is the SNR radius in parsec, and u_7 is the shock velocity in 10^7m s^{-1}. For Cas A, $u_7 = 0.6$ and $R_{pc} = 1.7$, giving $E_{max} \approx 60$ TeV for a typical interstellar magnetic field of 5 μG. Similarly for Tycho's SNR, $E_{max} \approx 130$ TeV, assuming $u_7 = 0.5$ and $R_{pc} = 4.3$ (following Williams et al. [67]). E_{max} falls far short of the knee for both these SNR, thus illustrating the challenge posted by Lagage and Cesarsky [36, 37] to DSA as an explanation of Galactic CR acceleration. These estimates of E_{max} are further reduced by a factor of three if the diffusion coefficient is set to $r_g c$ instead of the probably extreme $r_g c/3$ assumed above.

In the Sedov phase of SNR expansion, the radius increases, but the shock velocity decreases such that $\rho u^2 R^3 = 0.35\epsilon$, where ϵ is the energy of a Sedov blast wave expanding into a medium of density ρ. This implies that the maximum CR energy decreases during the Sedov phase: $E_{max} = 3 \times 10^{13} B_{\mu G} \epsilon_{44}^{1/2} n_e^{-1/2} R_{pc}^{-1/2}$ eV, where ϵ_{44} is in units of 10^{44} J and n_e is the ambient density in cubic centimetres. CR may be accelerated to a higher energy if they are able to stay with the shock throughout the Sedov phase and gain energy continually, but such high-energy CR are few in number because the probability of staying with the shock for a long time is very small, and their final energy is not much increased beyond their energy at the start of the Sedov phase.

The difficulties posed by Lagage and Cesarsky are clearly seen to be stringent when it is recognised that the Bohm diffusion coefficient $D = r_g c/3$ is a lower limit for CR diffusion along magnetic field lines. Two conditions must hold for the Bohm diffusion to apply. Firstly, fluctuations in the magnetic field δB must be at least comparable in magnitude with any mean field, $\delta B/B \geq 1$. Secondly, the scale length of the fluctuations must match the CR Larmor radius. CR barely notice fluctuations on a scale much smaller scale than the Larmor radius. On the other hand, if the scale length is much larger than the Larmor radius, the CR will see them as a mean field and spiral freely along the total field without scattering. However, a mixture of theoretical [49] and observational studies [59, 62] indicate that the assumption of the Bohm diffusion is not unreasonable.

3 Oblique and Perpendicular Shocks

According to Lagage and Cesarsky, the maximum CR energy is limited by the ratio of the cycle time τ_{cycle} to the age of the SNR. Jokipii [30] showed that the cycle time can be much shorter for 'perpendicular shocks' where the upstream magnetic field is perpendicular to the shock normal. In the intermediate case of an oblique shock with an angle θ between the magnetic field and the shock normal, a CR must propagate at a projected velocity $u/\cos\theta$ along a field line if it is to outrun the shock. Consequently, CR are overtaken by the shock in time $4D_u/(u/\cos\theta))$, the acceleration rate is increased by $1/\cos\theta$, and CR reach an energy which is higher by $1/\cos\theta$ in the same time R/u. This is still not sufficient to account for acceleration to a PeV unless θ is nearly $\pi/2$.

Acceleration can be most rapid when the shock is perpendicular ($\theta = \pi/2$). In this case, CR cannot outrun the shock by propagating along a field line, and CR must diffuse across magnetic field lines to penetrate into the upstream plasma. This is possible if CR are scattered by fluctuations in the magnetic field. In the standard theory for charged particle diffusion across a magnetic field, the cross-field diffusion coefficient is $D_\perp = D_{||}/(\omega_g \tau_{scat})^2$ where ω_g is the Larmor frequency, τ_{scat} is the scattering (collision) time for the CR in the perturbed magnetic field, and $D_{||}$ is the diffusion coefficient along the magnetic field. The CR acceleration rate is thereby increased by a factor $(\omega_g \tau_{scat})^2$ although acceleration ceases if $\omega_g \tau_{scat} > c/u$ in which case scattering is not sufficiently strong for CR to penetrate into the upstream plasma by one Larmor radius. Under optimal conditions and a suitable value of $\omega_g \tau_{scat}$, the maximum CR energy as defined by the acceleration time can be greatly increased [24, 30, 43].

Unfortunately, a different constraint intervenes to limit the maximum CR energy at a perpendicular shock. CR gain energy by drifting along the shock surface under the influence of the magnetic field discontinuity between the upstream magnetic field and the compressed downstream magnetic field. The source of the energy gain is the ordered $-\mathbf{u} \times \mathbf{B}$ electric field necessary for the thermal plasma to cross the magnetic field at velocity $\mathbf{u}$ in the rest frame of the shock. The maximum distance the CR can drift on the shock surface is the shock radius R yielding a maximum CR energy uBR which is very similar to the maximum CR energy gained at a parallel shock. If a SNR shock expands across a perpendicular magnetic field configured in the form

of a Parker spiral, uBR is the approximate electric potential between the pole and the equator of the SNR in the shock frame. It is possible to construct special CR trajectories in special magnetic field configurations for CR to gain higher energies, but these artificial cases are unlikely to be responsible for the acceleration of CR in large numbers. Although perpendicular shocks may be rapid CR accelerators, CR cannot reach PeV energies at SNR shocks propagating into fields of a few microgauss.

4 Magnetic Field Amplification

Apart from a numerical factor of order unity, the 'Hillas parameter' uBR provides a good estimate of the maximum CR energy where u, B, and R are the characteristic velocity, magnetic field and spatial scalelength, respectively. Hillas [28] surveyed a large range of putative CR acceleration sites with greatly varying values of B, u and R only to find that none of them stand out as the most likely source of high-energy CR. At one extreme, B and u are very large, but R is very small in pulsar magnetospheres. At the other extreme, R and u are very large, but B is very small in the lobes of radio galaxies.

Of the three quantities comprising the Hillas parameter, u and R are relatively fixed by shock kinetics and geometry. Only B is open to radical increase. It became apparent both observationally and theoretically in the early 2000s that the magnetic field can be amplified at high velocity shocks far beyond the unperturbed upstream value. Vink and Laming [64], Berezhko et al. [13] and Völk et al. [65] showed that amplified magnetic fields were needed to explain the thin strands of x-ray synchrotron emission coincident with the outer shocks of young supernova remnants. The essence of their analyses was that the thickness of the x-ray strand is determined by synchrotron losses. The fact that they are thin indicates that the electron synchrotron loss time is short, and the magnetic field must be large. The implied fields are of the order of 100s of microgauss downstream of the shock. The factor of ∼100 increase in magnetic field correspondingly increases the Hillas parameter by the same factor and may facilitate CR acceleration to a few PeV.

5 The Nonresonant Hybrid Instability

Coincidentally at the same time that amplified magnetic field was detected observationally in SNR, it was shown theoretically that there exists a plasma instability capable of amplifying magnetic field by orders of magnitude [8].

It had been recognised from the earliest papers on diffusive shock acceleration that the Alfven instability driven by CR streaming ahead of the shock could generate circularly polarised Alfven waves with wavelengths in spatial resonance with the CR Larmor radius. The spatially resonant Alfven waves strongly scatter the CR, thereby reducing the CR mean free path and diffusion coefficient and enabling diffusive shock acceleration. Because the instability relies upon a spatial resonance between the wavelength and the CR Larmor radius, it seemed unlikely that the instability would grow beyond $\delta B/B \sim 1$ since the resonance would then be destroyed. The instability might reduce the diffusion coefficient to the Bohm value if $\delta B/B \sim 1$, but would not increase the Hillas parameter and could not explain acceleration to PeV energies.

The nonlinear evolution of the magnetic field under the influence of CR streaming was investigated numerically by Lucek and Bell [40]. They coupled a particle simulation of initially streaming CR to a 3D magnetohydrodynamics (MHD) model of the background plasma. They found that the magnetic field grew by an order of magnitude beyond the initial value before scattering isotropised the streaming CR and removed the force driving instability. This suggested that CR streaming had the potential to increase the magnetic field and accelerate CR to higher energies. It was subsequently shown that the dominant instability is in fact not the resonant Alfven instability but the previously unrecognised nonresonant hybrid (NRH) instability [8]. Being nonresonant, there is less reason for the NRH instability to saturate at $\delta B/B \sim 1$. In some configurations, the linear analysis of its growth is in fact valid for large amplification of the magnetic field (e.g. Bell [9]).

The NRH instability can be understood by considering CR protons propagating with electric current $\mathbf{j}_0$ parallel to a magnetic field $\mathbf{B}_0$ in the z direction. Add a small magnetic field $\mathbf{B}_\perp$ ($B_\perp \ll B_0$) perpendicular to $\mathbf{B}_0$ with components in the (x, y) plane. If the wavelength $2\pi/k$ is much smaller than the CR Larmor radius, the CR trajectories are undeflected, and the current is unperturbed ($\mathbf{j}_1 = 0$). The equation of motion for the background thermal plasma with density ρ moving with velocity $\mathbf{u}_\perp$ in the perpendicular direction is

$$\rho \frac{\partial \mathbf{u}_\perp}{\partial t} = -\mathbf{j}_0 \times \mathbf{B}_\perp \,. \tag{2}$$

The density ρ is constant since the velocity is perpendicular to the z direction. The $-\mathbf{j}_0 \times \mathbf{B}_\perp$ force operates through the return current $-\mathbf{j}_0$ carried by the background plasma to balance the forward CR current. Alternatively, the force can be understood as the momentum-conserving reaction against the $\mathbf{j}_0 \times \mathbf{B}_\perp$ force acting on the CR. The magnetic field is frozen into the background plasma and evolves according to the ideal MHD equation:

$$\frac{\partial \mathbf{B}_\perp}{\partial t} = \nabla \times (\mathbf{u}_\perp \times \mathbf{B}_0) \tag{3}$$

Equations (2) and (3) can be manipulated to give

$$\frac{\partial B_x}{\partial t} = \frac{B_0 j_0}{\rho}\frac{\partial B_y}{\partial z} \qquad \frac{\partial B_y}{\partial t} = -\frac{B_0 j_0}{\rho}\frac{\partial B_x}{\partial z} \tag{4}$$

If $\mathbf{B}_\perp$ varies harmonically in the z direction parallel to $\mathbf{j}_0$ and $\mathbf{B}_0$ in proportion to $\exp(ikz)$, there exist purely growing circularly polarised modes with a growth rate

$$\gamma = \sqrt{\frac{kB_0 j_0}{\rho}}\,. \tag{5}$$

No approximations have been made in this derivation apart from the assumption that the wavelength is much smaller than the CR Larmor radius. The Larmor radius of a PeV proton in a microgauss magnetic field is 1 pc, so this is an acceptable assumption except that the scale length of the structure in the magnetic field must grow to a Larmor radius for effective CR scattering. Apart from the small wavelength assumption, the growth equation is valid for arbitrary nonlinearity, i.e. $B_\perp$ arbitrarily greater than B_0. This pure mode continues to grow indefinitely with growth rate γ. The same applies in some other special configurations [9]. In reality, the perturbed magnetic field more likely consists of a mixture of modes which interfere with each other nonlinearly and slow the growth rate, but a numerical simulation shows that the magnetic field can still be amplified by orders of magnitude [8].

The NRH instability differs from the Alfven instability in its polarisation. Both instabilities produce circularly polarised waves of helical magnetic field, but the polarisation rotates in opposite directions. In the Alfven instability, the magnetic field rotates in the same sense as the spiral CR trajectories to maintain a resonance between the magnetic field $\mathbf{B}_0$ and the streaming CR. In contrast, the NRH polarisation and the CR trajectories are counter-rotating and nonresonant. This surprising feature may explain why the NRH instability remained unrecognised for many years.

6 The Saturation of the NRH Instability

As shown by the graph of magnetic energy density against time in Fig. 1, the NRH instability can grow nonlinearly to amplify the magnetic field by a large factor. The instability continues to grow provided two conditions are satisfied. Firstly, the instability grows only if its characteristic scale length L does not exceed the CR Larmor radius; otherwise, CR spiral along the perturbed magnetic field lines and the $\mathbf{j}\times\mathbf{B}$ force averages to zero. Secondly, the $\mathbf{j}\times\mathbf{B}$ force driving the instability must exceed the magnetic tension $\mathbf{B}\times(\nabla\times\mathbf{B}/\mu_0)$ which opposes the expansion in the amplitude of spirals in the magnetic field. To order of magnitude, these two conditions are respectively $L < p/eB$ and $j > B/L\mu_0$. Eliminating L between the conditions gives $B^2/\mu_0 < Q_{\rm cr}/c$ where $Q_{\rm cr} = jpc/e$ is the energy flux carried by the CR in the rest frame of the background plasma. If $B^2/\mu_0 > Q_{\rm cr}/c$, either the scale length L must be larger than the CR Larmor radius, or L must be so short that the magnetic tension overpowers the $\mathbf{j}\times\mathbf{B}$ force.

Note that the resonant Alfven instability is not restricted in the same way by magnetic tension since the instability excites Alfven waves which are natural plasma modes and propagate without damping provided damping by collisions or wave-wave interactions can be neglected.

The NRH instability condition $B^2/\mu_0 < Q_{\rm cr}/c$ can be related to the CR energy density $U_{\rm cr}$. The upstream CR distribution is nearly at rest in the shock frame, so $Q_{\rm cr} = uU_{\rm cr}$ in the upstream frame. If $U_{\rm cr} = \eta\rho u^2$ where η is an efficiency factor, then the magnetic energy density is limited to $B^2/\mu_0 < \eta\rho u^3/c$.

We must be careful about the meaning we attach to the CR energy density $U_{\rm cr}$, the efficiency η and the magnetic energy density B^2/μ_0. The CR energy spectrum at a SNR shock extends by 6 orders of magnitude from GeV to PeV. A GeV proton has a Larmor radius 10^6 times smaller than that of a PeV proton, the scale height of its precursor ahead of the shock is correspondingly 10^6 times smaller, and it drives and responds to magnetic perturbations which are similarly 10^6 times smaller. Hence, the system of GeV CR and their accompanying magnetic fluctuations can be expected to decouple from that of PeV CR and their associated magnetic fluctuations. As a consequence, the discussion of $U_{\rm cr}$, η and B^2/μ_0 in the previous paragraph refers to a particular energy range of CR. Since CR energy densities are spread nearly equally between GeV and PeV, only a fraction $\sim 1/\log(10^6) \sim 0.07$ of the total CR energy density contributes to magnetic field amplification on a specified scale. If $\sim$30 % of ρu^2 is given to CR in total, then $U_{\rm cr} = \eta\rho u^2$ where $\eta \approx 0.3/\log(10^6) \approx 0.03$. Bell [8] and Bell et al. [12] give more detailed discussions of η. See also Zirakshvili and Ptuskin [69], although their parameter η_{esc} differs in definition by a numerical factor from our η. The magnetic energy density associated with a particle energy range of CR is then $B^2/\mu_0 \approx \eta\rho u^3/c$ with $\eta \approx 0.03$. This provides an estimate of a magnetic field $B = 160 n_e^{1/2} u_7^{3/2}$ ∝G available to scatter CR in a particular energy range.

The magnetic field is amplified on a range of scales corresponding to the Larmor radii of CR with energies ranging from GeV to PeV, in which case the total magnetic energy density immediately upstream of the shock is better estimated by setting $\eta \approx 0.3$ giving $B = 500 n_e^{1/2} u_7^{3/2}$ ∝G. The field is compressed by a further factor of about 3 when it passes through the shock to give a good match to the magnetic field inferred from the observed x-ray synchrotron emission at SNR shocks.

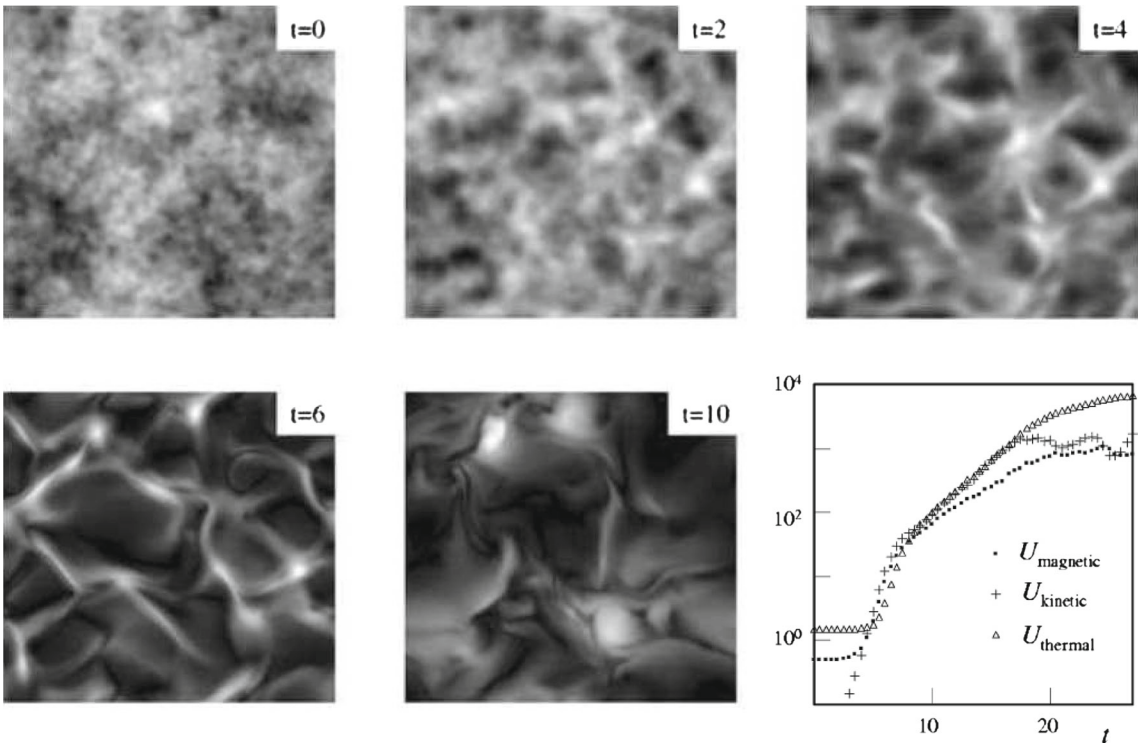

Fig. 1 Plots of the magnitude of a magnetic field driven by CR streaming into the page (2D slices of a 3D simulation). The field grows from noise on a small spatial scale at $t = 0$. By $t = 10$, the spatial scale has grown to the size of the computational box. The graph shows how the mean magnetic, kinetic and thermal energy densities increase with time. This figure is composed from Figs. 3 and 4 of Bell [8] where further details can be found. The units of time are such that $\gamma_{\max} = 1.26$

7 NRH Scale Lengths

For the NRH instability to explain CR acceleration to PeV, it must not only amplify the magnetic field sufficiently but also produce magnetic structures on the scale of the CR Larmor radius. The growth rate is proportional to $\sqrt{k}$, so small-scale structure grows most rapidly. Fortunately, magnetic field amplification and increase in spatial scale length are connected aspects of the nonlinear NRH instability since the field grows by the stretching of field lines. In its simplest configurations, the magnetic field is amplified by an increase in the radius of loops of magnetic field or in the radius of a helical field line. Equation (3) for a harmonic mode with wavenumber k can be integrated to show that the radius of spirals in the magnetic field is $r \sim k^{-1} B_\perp / B_0$, which indicates that the scale length grows nonlinearly in proportion to the magnetic field.

Nonlinear numerical simulations presented in the grayscale plots of Fig. 1 (see also Reville et al. [49], Zirakashvili et al. [70], Riquelme and Spitkovsky [51, 52], and Reville and Bell [48]) clearly demonstrate strong growth in scale. The instability evolves nonlinearly into a series of expanding cells consisting of walls of high plasma density and strong magnetic field spiralling around cavities of low density and low magnetic field. As discussed in the previous section, the instability grows over a range of wavenumbers bounded by $k > r_g^{-1}$ at a long wavelength and $kB < \mu_0 j$ at a short wavelength. Saturation occurs when these two wavenumbers coincide with both $k \sim r_g^{-1}$ and $kB \sim \mu_0 j$. Consequently, $kr_g \sim 1$ at saturation and the dominant scale length at saturation is equal to the CR Larmor radius as required for effective CR scattering.

8 NRH Growth Times

As shown above, the NRH instability has the capacity to amplify the magnetic field by orders of magnitude. We now investigate the conditions necessary for the instability to grow through many e-foldings in the available time. The NRH growth time is

$$\gamma^{-1} = 3 \times 10^4 (kr_g)^{-1/2} u_7^{-3/2} E_{\mathrm{PeV}} B_{\mu\mathrm{G}}^{-1} \eta_{0.03}^{-1/2} \ \mathrm{yr} \qquad (6)$$

where E_{PeV} is the energy of CR protons in PeV and $\eta_{0.03}$ is η relative to 0.03 ($\eta_{0.03} = 1$ if $\eta = 0.03$). Equation (6) shows that the NRH instability does not have time to grow on the scale of the Larmor radius ($kr_g \sim 1$) of a PeV proton in young SNR. Fortunately, the growth rate is proportional to $\sqrt{k}$, so there is time for the instability to grow initially

on a small scale ($kr_g \gg 1$) and subsequently expand nonlinearly to match the CR Larmor radius. The smallest scale length on which the instability can grow is set by the tension in the magnetic field. As discussed above, the $\mathbf{j} \times \mathbf{B}$ must dominate the magnetic force $\mathbf{B} \times (\nabla \times \mathbf{B})/\mu_0 \sim kB^2/\mu_0$, and this condition is satisfied if $k < \mu_0 j/B$. The growth rate is at a maximum $\gamma_{\max} = 0.5j\sqrt{\mu_0/\rho}$ when the wavenumber is $k_{\max} = 0.5\mu_0 j/B$ [8]. The corresponding fastest growth time and associated scale length are

$$\gamma_{\max}^{-1} = 40 n_e^{-1/2} u_7^{-3} E_{\mathrm{PeV}} \eta_{0.03}^{-1} \text{ yr} \tag{7}$$

$$k_{\max}^{-1} = 3 \times 10^{12} n_e^{-1} u_7^{-3} E_{\mathrm{PeV}} B_{\mu\mathrm{G}} \eta_{0.03}^{-1} \text{ m} \tag{8}$$

giving

$$k_{\max} r_g = 10^4 \eta_{0.03} n_e u_7^3 B_{\mu\mathrm{G}}^{-2} \tag{9}$$

The growth time $\gamma_{\max}^{-1}$ of the fastest growing mode is sufficiently short to allow many e-foldings during the lifetime of a SNR. The initial scale length $k_{\max}^{-1}$ is much smaller than the CR Larmor radius, but $k_{\max}^{-1}$ increases in proportion to the growing magnetic field. $k_{\max} r_g \propto B^{-2}$, so an increase in magnetic field from a few microgauss to ~100 μG increases $k_{\max} r_g$ to ~1 as required for effective CR scattering.

9 $E_{\max}$ as Determined by NRH Growth Times

As seen in the grey-scale plots in Fig. 1, magnetic field structures grow substantially in a few growth times. The graph of magnetic energy density in Fig. 1 shows that the magnetic field grows substantially in the same time. In this section, we take $\tau_{\mathrm{amp}} = 5\gamma_{\max}^{-1}$ to be the characteristic time for magnetic field amplification as observed in young SNR. As shown in Section 8 of Bell et al. [12], $E_{\max}$ for a spherical freely expanding blast wave can be calculated by equating τ_{amp} to $R/2u$. Equation (7) can be inverted to derive an equation for the maximum CR energy:

$$E_{\max} = 230 n_e^{1/2} u_7^2 R_{\mathrm{pc}} \eta_{0.03} \text{ TeV} \tag{10}$$

An equivalent result was first derived by Zirakashvili and Ptuskin [69] using a more sophisticated model for CR transport and acceleration. The physics underlying their calculation of the maximum CR energy is the same in essence.

Equation (10) for the maximum CR energy is governed by the NRH growth rate. If CR were accelerated to a higher energy, the upstream CR electric current driving the instability would be reduced for the same CR energy flux $\eta\rho u^3$ since fewer CR would be needed to carry the CR energy. Conversely, if CR were accelerated only to a lower energy, the CR electric current would be increased, the growth rate would increase and the magnetic field would be amplified sufficiently to accelerate CR to the higher energy. Hence, the CR current and the NRH growth are self-regulated to drive the instability through about five e-foldings ($\tau_{\mathrm{amp}} \approx 5\gamma_{\max}^{-1}$) in the time available. Note that the magnitude of the magnetic field does not appear in this derivation of $E_{\max}$.

It immediately stands out that $E_{\max}$ in (10) falls short of the energy of the knee for parameters appropriate to young SNR. Our derivation of $E_{\max}$ is approximate, for example, in the estimation that $\tau_{\mathrm{amp}} = 5\gamma_{\max}^{-1}$. From Fig. 1, it appears that if anything a time greater than $5\gamma_{\max}^{-1}$ should be allowed for magnetic field amplification, in which case $E_{\max}$ would be lower and acceleration to PeV less likely. On the other hand, there are ways in which the value for $E_{\max}$ given in (10) might be an underestimate. For example, our derivation treats CR as mono-energetic. Lower energy CR may be leaking upstream from the shock to add to the electric current driving magnetic field amplification.

Equation (10) gives $E_{\max} \sim$ 100–200 TeV for the historical SNR since their velocities are ~5,000 km s^{-1} or less, which is a full factor of 10 lower than the CR energy at the knee. The CR energies reached in the historical SNR and the implications for Galactic CR origins are discussed below in Section 14.

10 CR Escape Upstream is Essential

Here we emphasise that CR acceleration only occurs if CR accelerated to the highest energy escape upstream of the shock in contrast to CR accelerated to lower energies which are advected away downstream of the shock.

Consider a point ahead of the approaching shock. CR streaming away from the shock pass freely through this point until the instability has grown sufficiently to scatter CR and confine them to the shock precursor. In accord with the discussion above, this occurs when $\int \gamma_{\max} dt \sim 5$ where $\gamma_{\max} = 0.5j\sqrt{\mu_0/\rho}$. Consequently, confinement sets in when the time integral of CR charge per unit area passing through this point reaches

$$q_{\mathrm{cr}} = \int j dt \sim 10\sqrt{\rho/\mu_0} \tag{11}$$

The condition for confinement is that a charge q_{cr} per unit area of shock must escape freely upstream before CR following after it can be confined. Hence, CR escape upstream is an essential feature of CR acceleration by shocks.

11 The Shock Velocity at which the NRH Instability Switches Off

The NRH instability operates (i) only on scales comparable or smaller than the Larmor radius of the CR with energy E (in eV) driving the instability (i.e. $k > cB/E$), and (ii) only

if the $\mathbf{j} \times \mathbf{B}$ force driving magnetic field amplification is stronger than the magnetic force $\mathbf{B} \times (\nabla \times \mathbf{B})/\mu_0$ (i.e. $k < \mu_0 j/B$). Consequently, there is no range of wavelengths at which the NRH instability is active if $\mu_0 j/B < cB/E$, (i.e. $j < cB^2/\mu_0 E$). Since the CR energy flux is $jE = \eta\rho u^3$, the condition for magnetic field amplification by the NRH instability is $u > (cB^2/\eta\rho\mu_0)^{1/3}$, which is equivalent to

$$u > 350 B_{\infty\mathrm{G}}^{2/3} \eta_{0.03}^{-1/3} n_e^{-1/3} \text{ km s}^{-1} \tag{12}$$

This limit implies that the NRH instability is active in the historical SNR which are expanding at ∼5,000 km s^{-1}, but that it is unavailable for magnetic field amplification during much of the Sedov phase. When the expansion drops below about 1,000 km s^{-1}, the $\mathbf{j} \times \mathbf{B}$ force is too weak to overcome the magnetic force $\mathbf{B} \times (\nabla \times \mathbf{B})/\mu_0$ for magnetic fields of a few μG. This condition (12) is equivalent to requiring that the saturation magnetic field derived in Section 6 must be greater than the initial magnetic field in the ambient medium. It does not apply to the Alfven instability where the magnetic force is part of the natural oscillation of the Alfven waves excited by the instability as mentioned in Section 6.

12 The Alfven Instability

As shown above, the NRH instability at the outer shocks of SNR is only excited in the early stages of evolution when the expansion velocity is comparable with or greater than ∼1,000 km s^{-1} for an ambient magnetic field of a few microgauss. Below this velocity, the resonant Alfven instability is dominant.

From (6) and (7) in Bell [8], the dispersion relation including both the NRH and Alfven instabilities for a mono-energetic CR distribution drifting diffusively at the shock velocity u is

$$\omega^2 = k^2 v_\mathrm{A}^2 - \frac{kjB}{\rho} \times \left\{ 1 - \frac{3}{2k^2 r_g^2} + \frac{3}{4} \frac{1 - k^2 r_g^2}{k^3 r_g^3} \times \left[i\pi + \log\left(\frac{kr_g + 1}{kr_g - 1} \right) \right] \right\} \tag{13}$$

where r_g is the CR Larmor radius and the imaginary term on the right-hand side is cancelled when $kr_g < 1$ by the imaginary part of the logarithmic term. The combination of the quantities kjB shows the importance of the relative directions of CR current, the magnetic field and the polarisation of the wave. Changing the sign of j while keeping k and B unchanged causes an unstable wave to become stable and vice versa under most circumstances. See Bell [8] for more details.

In the limit of large j appropriate to young SNR, the NRH instability grows most strongly at wavelengths shorter than the CR Larmor radius ($kr_g \gg 1$) where the dispersion relation reduces to

$$\omega^2 = k^2 v_\mathrm{A}^2 - \frac{kjB}{\rho} \tag{14}$$

and the term $k^2 v_\mathrm{A}^2$ sets the short wavelength limit beyond which the magnetic tension is stabilising.

In the limit of small j ($jB/\rho \ll v_\mathrm{A}^2/r_g$) appropriate to old SNR and growth of the Alfven instability, the dispersion relation reduces to

$$\omega^2 = k^2 v_\mathrm{A}^2 + \frac{3\pi i}{4} \frac{kjB}{\rho} \frac{k^2 r_g^2 - 1}{k^3 r_g^3} \tag{15}$$

The maximum instability growth rate of the Alfven instability is

$$\gamma_{\mathrm{A,max}} = \frac{\pi}{4\sqrt{3}} j \sqrt{\frac{\mu_0}{\rho}} \tag{16}$$

which occurs when the wavelength of the Alfven wave is $3.6 r_g$ ($kr_g = \sqrt{3}$).

The growth of the Alfven instability is governed by the imaginary term ($i\pi$) in the square brackets in (13) in contrast to the growth of the NRH which is determined by the first term since fastest NRH growth occurs when $kr_g >> 1$. The Alfven instability is driven by $\mathbf{j}_1 \times \mathbf{B}_0$ where $\mathbf{j}_1$ is the perturbed CR current and $\mathbf{B}_0$ is the unperturbed magnetic field, whereas the NRH instability is driven by $\mathbf{j}_0 \times \mathbf{B}_1$. The two instabilities also differ in their polarisation and dominant wavenumber: $kr_g \approx 1$ for the Alfven instability compared with $kr_g > 1$ for the fastest growing NRH wavelength. Both instabilities have nearly the same maximum growth rate, but each dominates under different conditions. The crossover from the Alfven to the NRH instability occurs when the CR current j becomes large enough for kjB/ρ to exceed $k^2 v_\mathrm{A}^2$ on the Larmor scale ($kr_g \sim 1$) at which point the $\mathbf{j} \times \mathbf{B}$ force overpowers the tension in the magnetic field on the scale of a CR Larmor radius.

The similar values of the Alfven and NRH maximum growth rates, as pointed out by Zirakashvili and Ptuskin [69], allows the analysis of Section 9 to be applied at low shock velocities relevant to older SNR as well as to high-velocity young SNR shocks at which the NRH instability is active. Equation (10) is therefore applicable to both young SNR and SNR throughout the Sedov phase.

Equation (10) finally becomes inapplicable when the shock velocity drops to a few times the Alfven speed, $v_\mathrm{A} = 2 B_{\infty\mathrm{G}} n_e^{-1/2} \text{km s}^{-1}$ since the Alfven instability is driven by the drift of CR relative to the motion of the the driven resonant Alfven wave. However, the shock may have dissipated by that time if the shock velocity has dropped below the ion acoustic sound speed, $c_s = 13 T_{eV}^{1/2}$ km s^{-1}.

13 Spectrum of Escaping CR

Since the maximum growth rates of both the NRH and the Alfven instabilities are the same to that within a numerical factor close to one, (10) for the energy $E_{\max}$ of escaping CR can be applied throughout the lifetime of a SNR. By definition of η, the energy flux of CR escaping with energy $E_{\max}$ is $\eta\rho u^3$, and the total energy spectrum of CR injected into the Galaxy by a SNR can be derived.

The number $N(E)$ of CR escaping with energy greater than E is the number of CR escaping before the SNR radius expands to a radius R at which $E_{\max} = E$.

$$N(E) = \int_0^R 4\pi R^2 \frac{\eta\rho u^2}{E} dR \tag{17}$$

The corresponding differential energy spectrum $n(E) = -dN/dE$ is

$$n(E) = -4\pi R^2 \frac{\eta\rho u^2}{E} \frac{dR}{dE} \tag{18}$$

From (10), $E \propto Ru^2$ for a uniform ambient density. In the self-similar Sedov phase $u^2 \propto R^{-3}$, so the spectrum of CR escaping into the interstellar medium in the Sedov phase is

$$n(E) \propto E^{-2} \tag{19}$$

which is the same as the spectrum for test particle CR accelerated at a strong shock. This is not surprising since the same E^{-2} spectrum of escaping CR can arise under a range of self-similar assumptions regarding CR escape during the Sedov phase [20, 22, 44]. It is sufficient (from (18)) that the dependence of the CR escape energy on shock radius should be a power law and that the efficiency η should be constant.

The energy of a Sedov blast wave of radius R expanding into a medium with $\gamma = 5/3$ and density ρ at velocity u is approximately $3\rho R^3 u^2$ with the consequence from (10) that the energy of CR escaping at a particular stage of a Sedov expansion is

$$E = 5M_{\rm A}^{4/3}\epsilon_{44}^{1/3}B_{\mu\rm G}^{4/3}n_e^{-1/2}\text{GeV} \tag{20}$$

where the expansion velocity is given in terms of the Alfven Mach number $M_{\rm A}$ of the shock, ϵ_{44} is the blast wave energy in 10^{44} J, and $B_{\mu\rm G}$ is the ambient magnetic field in microgauss. The shock dissipates into the interstellar medium as $M_{\rm A} \to 1$ at which time CR are no longer confined to the remnant since the magnetic fluctuations that scatter them move at the Alfven speed. Assuming that CR acceleration weakens when $M_{\rm A} \sim 3$ at a shock propagating into a field of 5 μG, the energy spectrum of escaping CR terminates at a lower energy of $E_{\min} \sim 200$ GeV. At this point, CR previously confined to the interior of the SNR are released into the interstellar medium.

Galactic CR accelerated by SNR can be divided into two populations: (i) CR above $E_{\min} \sim 200$ GeV that escape upstream during SNR expansion and (ii) CR at energies below $E_{\min}$, but also extending into the TeV range, which are advected into the interior of the SNR and released into the ISM at the end of SNR expansion when the shock dissipates.

For the different reasons explained above, both populations have the same energy spectrum $\propto E^{-2}$ at source, although in reality additional factors might be expected to slightly steepen or flatten each spectrum, and propagation losses steepen the entire spectrum to the approximately $E^{-2.7}$ power law arriving at the Earth. It is unlikely that the spectra of the two populations should join smoothly at $E_{\min}$ without at least a slight bend in the spectrum or some noticeable feature. The most obvious candidate for a spectral signature of a join in the spectrum is that seen by PAMELA at about 200 GeV [1]. The observational status of the detailed spectral feature is uncertain in the light of recent AMS observations [60], but a change in spectral index near this energy is supported by other measurements [5]. Also our theoretical estimate of 200 GeV as the exact value of $E_{\min}$ is subject to considerable uncertainty, and energy-dependent CR propagation might be an alternative explanation for a change in spectral index [17, 61].

The total energy in escaping CR can be derived from the current $j_{\rm cr}$ of escaping CR as discussed above (17) and (18). Only the highest energy CR being accelerated escape at any one time. They carry only ~10 % of the energy content of the CR carried into the interior of the SNR. CR carried into the interior cool adiabatically as the SNR expands. Their energy is recouped as their pressure drives the shock and accelerates later generations of CR. Integration over the whole lifetime of the SNR shows overall that the acceleration and release of CR into the interstellar medium can be a highly efficient process [12].

14 Can SNR Accelerate CR to the Knee?

The expression $E_{\max} = 230 n_e^{1/2} u_7^2 R_{\rm pc}$ TeV, derived in Section 9, (10), for the maximum CR energy can be applied to the historical SNR usually regarded as the most likely source of PeV CR in the Galaxy. Similar results are obtained by Zirakashvili and Ptuskin [69]. The controlling parameters, n_e, u_7 and $R_{\rm pc}$ are often uncertain, particularly the ambient density n_e, but also the radius $R_{\rm pc}$ since the distance to the SNR is not always well determined. The predicted maximum CR energies in TeV are as follows [46, 63, 67]:

Cas A: 160 ($n_e = 2$, $R_{\rm pc} = 2$ and $u_7 = 0.5$)
SN1006: 100 ($n_e = 0.3$, $R_{\rm pc} = 9$ and $u_7 = 0.3$)
Tycho: 100 ($n_e = 0.2$, $R_{\rm pc} = 4$ and $u_7 = 0.5$)
Kepler: 70 ($n_e = 1$, $R_{\rm pc} = 2$ and $u_7 = 0.4$)

The maximum CR energy is low in each case because the expansion is already heavily decelerated. If we replace the

current expansion velocity with the mean expansion velocity $\bar{u}_7 = R_{\rm pc}/t_{100}$ where t_{100} is the age in hundreds of years, such that (10) becomes $E_{\rm max} = 230 n_e^{1/2} R_{\rm pc}^3 t_{100}^{-2}$ TeV, then the estimated maximum CR energies are larger:

Cas A: 240 ($n_e = 2$, $R_{\rm pc} = 2$ and $t_{100} = 3.3$)
SN1006: 900 ($n_e = 0.3$, $R_{\rm pc} = 9$ and $t_{100} = 10$)
Tycho: 540 ($n_e = 0.5$, $R_{\rm pc} = 4$ and $t_{100} = 4.4$)
Kepler: 120 ($n_e = 1$, $R_{\rm pc} = 2$ and $t_{100} = 4$)

The mean expansion velocity predicts a higher CR energy in each case, approaching 1 PeV for SN1006 because of its high average expansion velocity. However, the predicted CR energy depends on the third power of the radius and, hence, distance to the SNR. The derived distances to Tycho and Kepler vary by a factor of two between the largest and the smallest, so the uncertainties are very large in the above CR energies. Moreover, (10) might easily be in error by a factor of 2 or 3 because of the assumptions entering its derivation as discussed in Section 9. Most of the assumptions made in the derivation of (10) were generous in terms of trying to make $E_{\rm max}$ larger rather than smaller so as to reach the knee. For example, it is easy to see how the efficiency parameter η might be smaller than 0.03, but not much larger than this (but see Schure and Bell [55]). Nevertheless, the CR energies predicted for present expansion velocities fall substantially short of the energy of the knee, so it appears likely that none of the historical SNR are, at present, accelerating CR to the knee.

The dependence of $E_{\rm max}$ on the square of the shock velocity implies that the highest CR energies are more probably reached in young high-velocity SNR. The youngest known Galactic SNR, G1.9 + 0.3 aged 110 years, is expanding at 18,000 km s^{-1} with a radius of 2.2 pc [18]. Reynolds et al. [50] give an ambient density of 0.04 cm^{-3} predicting a maximum CR energy $E_{\rm max} = 330$ TeV from (10). If the SNR were expanding at the same velocity into a higher-density circumstellar medium, 1 cm^{-3} for example, it could be accelerating CR to the knee.

However uncertain the above estimates for $E_{\rm max}$, the strong dependence on expansion velocity points to the ideal PeV accelerator as a very young SNR expanding at a high velocity into a dense wind environment as previously suggested by Völk and Biermann [66] and Bell and Lucek [11]. Ptuskin et al. [45] survey different types of supernovae and find that type IIb SN may accelerate CR to a particularly high energy and may accelerate iron to 5×10^{18} eV. SN1987A may be a relatively nearby and well-diagnosed example of a high-energy accelerator. Constant expansion for time $t_{\rm yr}$ in years at its initial expansion velocity of 35,000 km s^{-1} predicts $E_{\rm max} = 100 t_{\rm yr} n_e^{1/2}$ TeV. Expansion into a high-density circumstellar medium over a decade or more should accelerate CR to the knee quite easily, and possibly to higher energies. SN1987a has passed through a number of different phases since it exploded into a highly structured medium including rings of radius 0.2 pc and with a range of densities $\sim (1-30) \times 10^3$ cm^{-3} [42]. The ejecta velocity slowed to 7,000 km s^{-1} on encountering the dense ring [38]. Substituting $u_7 = 0.7$, $n_e = 10^4$ and $R_{\rm pc} = 0.2$ in (10) predicts an estimated maximum CR energy at that stage of $E_{\rm max} = 2$ PeV. The ring has a mass of ~0.06 solar masses [42], so the energy processed through the shock during the encounter with the ring is $\sim 3 \times 10^{42}$ J which would contribute substantially to the Galactic CR energy budget if a similar SNR occurred in the Galaxy.

It appears that very young SNR are the most likely sites for acceleration to the knee. Schure and Bell [54] have analysed the evolution of the CR spectrum in the pre-Sedov phase for SNR expanding into a pre-ejected circumstellar wind. They find that Cas A probably accelerated CR to PeV energies at an earlier stage of its expansion. If acceleration to the knee only happens where SNR expand into a dense wind, then the CR composition can be expected to be heavier at energies approaching the knee. This would be consistent with the observation that the Galactic helium spectrum is flatter than the proton spectrum and that helium nuclei are more numerous than protons at the knee [32].

15 Conclusion

Cosmic ray physics is now solidly part of mainstream astrophysics, particularly as a result of x-ray and γ-ray observations of in situ CR acceleration. Theoretical models of Galactic CR acceleration to PeV energies can be constructed with the tentative conclusion that CR are accelerated to the knee in very young SNR and that probably none of the known Galactic SNR are able to accelerate protons beyond a PeV at the present time. Measurements of CR composition and precise determinations of the detailed energy spectra of different species increasingly provide powerful tests of theory. Observations with the CTA Cherenkov telescope [2, 29] should decisively indicate whether our current models are on the right lines.

Acknowledgments I thank Brian Reville, Klara Schure and Gwenael Giacinti for many insightful discussions on cosmic ray and related physics. The research leading to this review has received funding from the European Research Council under the European Community's Seventh Framework Programme (FP7/2007-2013)/ERC grant agreement no. 247039 and from grant number ST/H001948/1 made by the UK Science Technology and Facilities Council.

References

1. O. Adriani, et al., Sci. **332**, 69 (2011)

2. F. Aharonian, Astropart. Phys. **43**, 71 (2013)
3. F. Aharonian, et al., A&A. **464**, 235 (2007)
4. F. Aharonian, et al., A&A. **531**, C1 (2011)
5. H.S. Ahn, et al., ApJLett. **714**, L89 (2010)
6. W.I. Axford, E. Leer, G. Skadron, Proc. 15th ICRC (Plovdiv.) **11**, 132 (1977)
7. A.R. Bell, MNRAS. **182**, 147 (1978)
8. A.R. Bell, MNRAS. **353**, 550 (2004)
9. A.R. Bell, MNRAS. **358**, 181 (2005)
10. A.R. Bell, Astropart. Phys. **43**, 56 (2013)
11. A.R. Bell, S.G. Lucek, MNRAS. **321**, 433 (2001)
12. A.R. Bell, K.M. Schure, B. Reville, G. Giacinti, MNRAS. **431**, 415 (2013)
13. E.G. Berezhko, L.T. Ksenofontov, H.J. Völk, A&A. **412**, L11 (2003)
14. R.D. Blandford, D. Eichler, Phys. Rep. **154**, 1 (1987)
15. R.D. Blandford, J.P. Ostriker, ApJ. **221**, L29 (1978)
16. P. Blasi, E. Amato, JCAP01. **2012**, 011 (2012)
17. P. Blasi, E. Amato, P.D. Serpico, Phys. Rev. Lett. **109**, 061101 (2012)
18. K.J. Borkowski, S.P. Reynolds, U. Hwang, D.A. Green, R. Petre, K. Krishnamurthy, R. Willett, ApJL. **771**, 9 (2013)
19. A.M. Bykov, S.M. Osipov, D.C. Ellison, MNRAS. **410**, 39 (2011)
20. D. Caprioli, P. Blasi, E. Amato, Astropart. Phys. **33**, 160 (2010)
21. L.O'C. Drury, Rep. Prog. Phys. **46**, 973 (1983)
22. L.O'C. Drury, MNRAS. **415**, 1807 (2011)
23. L.O'C. Drury, S.A.E.G. Falle, MNRAS. **222**, 353 (1986)
24. D.C. Ellison, M.G. Baring, F.C. Jones, ApJ. **453**, 873 (1995)
25. E. Fermi, Phys. Rev. **75**, 1169 (1949)
26. J. Giacalone, J.R. Jokipii, ApJL. **663**, L41 (2007)
27. F. Guo, S. Li, H. Li, J. Giacalone, J.R. Jokipii, D. Li, ApJ. **747**, 98 (2012)
28. A.M. Hillas, ARA&A. **22**, 425 (1984)
29. J.A. Hinton, W. Hofmann, ARA&A. **47**, 523 (2009)
30. J.R. Jokipii, ApJ. **313**, 842 (1987)
31. F.C. Jones, D.C. Ellison, Space Sci. Rev. **58**, 259 (1991)
32. K.-H. Kampert, Nucl. Phys. B Proc. Supp. **165**, 294 (2007)
33. G.F. Krymsky, Sov. Phys. Dokl. **22**, 327 (1977)
34. G.F. Krymsky, et al., Proc. 16th ICRC (Kyoto). **2**, 39 (1979)
35. R. Kulsrud, W.P. Pearce, ApJ. **156**, 445 (1969)
36. O. Lagage, C.J. Cesarsky, A&A. **118**, 223 (1983a)
37. O. Lagage, C.J. Cesarsky, ApJ. **125**, 249 (1983b)
38. J. Larsson, et al., Nat. **474**, 484 (2011)
39. I. Lerche, ApJ. **147**, 689 (1967)
40. S.G. Lucek, A.R. Bell, MNRAS. **314**, 65 (2000)
41. M.A. Malkov, L.O'C. Drury, Rep. Prog. Phys. **64**, 429 (2001)
42. S. Mattila, et al., ApJ. **717**, 1140 (2010)
43. A. Meli, P.L. Biermann, A&A. **454**, 687 (2006)
44. Y. Ohira, K. Mirase, R. Yamazaki, A&A. **513**, A17 (2010)
45. V.S. Ptuskin, V.N. Zirakashvili, E.-S. Seo, ApJ. **718**, 32 (2010)
46. J.C. Raymond, et al. ApJ. **659**, 1257 (2007)
47. B. Reville, A.R. Bell, MNRAS. **419**, 2433 (2012)
48. B. Reville, A.R. Bell, MNRAS. **430**, 2873 (2013)
49. B. Reville, S. O'Sullivan, P. Duffy, J.G. Kirk, MNRAS. **386**, 509 (2008)
50. S.P. Reynolds, K.J. Borkowski, D.A. Green, U. Hwang, I. Harrus, R. Petre, ApJL. **680**, L41 (2008)
51. M. Riquelme, A. Spitkovsky, ApJ. **694**, 626 (2009)
52. M. Riquelme, A. Spitkovsky, ApJ. **717**, 1054 (2010)
53. K.M. Schure, A.R. Bell, MNRAS. **418**, 782 (2011)
54. K.M. Schure, A.R. Bell, MNRAS. **435**, 1174 (2013a)
55. K.M. Schure, A.R. Bell, MNRAS. **437**, 2802 (2014)
56. Skilling, MNRAS. **172**, 55 (1975a)
57. Skilling, MNRAS. **173**, 245 (1975b)
58. Skilling, MNRAS. **173**, 255 (1975c)
59. M.D. Stage, G.E. Allen, J.C. Houck, J.E. Davis, Nat. Phys. **2**, 614 (2006)
60. S. Ting, The AMS spectrometer on the International Space Station, Highlight Talk, ICRC 2013 (2013)
61. N. Tomassetti, ApJL. **752**, L13 (2012)
62. Y. Uchiyama et al., Nat. **449**, 576 (2007)
63. J. Vink, ApJ. **689**, 231 (2008)
64. J. Vink, J.M. Laming, ApJ. **584**, 758 (2003)
65. H.J. Völk, E.G. Berezhko, L.T. Ksenofontov, A&A. **433**, 229 (2005)
66. H.J. Völk, P. Biermann, ApJL. **333**, L65 (1988)
67. B.J. Williams et al., ApJ. **770**, 129 (2013)
68. D.G. Wentzel, ARA&A. **12**, 71 (1974)
69. V.N. Zirakashvili, V.S. Ptuskin, ApJ. **678**, 939 (2008)
70. V.N. Zirakashvili, V.S. Ptuskin, H.J. Völk, ApJ. **678**, 255 (2008)